Signal, Image and Video Processing manuscript No.
(will be inserted by the editor)

Body Temperature Measurement of an Animal by Tracking in Biomedical Experiments

Guillaume-Alexandre Bilodeau · Sébastien Desgent · Rana Farah · Sandra Duss · J.M. Pierre Langlois · Lionel Carmant

Received: date / Accepted: date

Abstract In this paper, we present a method to measure the body temperature of an animal using a thermographic camera in hyperthermia experiments, where the heat contrast between the animal and its background is low. This work was done in the context of the study of artificially induced atypical febrile seizures. In order to measure the temperature of a moving animal continuously, we need to detect it in each video frame, and then select a subset of pixels to evaluate its body temperature. To detect the animal in each frame, we propose a tracking method based on the minimization of a cost function that uses constraints such as

G.A. Bilodeau · R. Farah · J.M.P. Langlois

Department of Computer and Software Engineering,

École Polytechnique de Montréal,

P.O. Box 6079, Station Centre-ville Montréal (Québec), Canada, H3C 3A7,

E-mail: {guillaume-alexandre.bilodeau, rana.farah, pierre.langlois}@polymtl.ca

S. Desgent · S. Duss · L. Carmant

Centre de Recherche du Centre Hospitalier Universitaire Sainte-Justine, 3175, Côte Ste-Catherine, Montréal, (Québec), Canada, H3T 1C5,

E-mail: sdesgent@gmail.com, duss.sandra@gmail.com, lionel.carmant@umontreal.ca

temperature smoothness and proximity. The temperature of the animal is then taken as the mean of a subset of pixels from the detected area. For videos up to 19000 frames long, the method achieves temperature estimation within 0.7^oC from ground-truth more than 73% of the time in difficult measurement scenarios.

Keywords Thermography · Body temperature measurement · Hyperthermia · Seizures · Animal tracking · Low contrast

1 Introduction

Atypical febrile seizures (prolonged, lateralized, or repetitive seizures with fever) have important clinical implications because of their recognized association with the mesial temporal lobe epilepsy syndrome (MTLE), which is the most common of intractable epilepsies. Retrospective studies suggest that between 30% and 60% of patients with MTLE have histories of atypical febrile seizures occurring early in childhood [1, 2]. Despite these findings, the events that lead to atypical febrile seizures remain poorly understood, and the suggested risk factors for this condition, which include neurologic and/or perinatal abnormalities, early-life stress and a low threshold temperature at the onset of convulsions, have yet to be validated with animal models.

Thus, the development of an animal model of febrile seizures is a critical step in understanding the progression from febrile seizures to MTLE. In that trend and during the past ten years, researchers have developed animal models based on a two-hit hypothesis where an early-life insult, such as the combination of an artificial cortical lesion (e.g. microgyria) one day after birth (P1) or the induction of chronic early-life stress during the first nine days of life (e.g. daily cortisol administration) followed by prolonged hyperthermic febrile seizures occurring later at P10 in early postnatal life, lead to predisposition to temporal lobe epilepsy

in adult male rats [3, 4, 5, 6, 7, 8, 9]. In that model, the P10 animals are subjected to a hyperthermia experiment where their core temperature is increased to 44-47^{o}C by experimentally circulating hot-dry air around their body to provoke a generalized convulsion (GC) [5]. This hyperthermia experimental approach mimics the human fever condition and can be justified for two main reasons: 1) Hyperthermia without fever also causes seizures in children and 2) in infant rats, fever and hyperthermia utilize common immune mechanisms to elicit seizures, namely the production of the pyrogenic cytokine IL-1 within the hippocampus [10]. Previous experiments using a rectal probe during hyperthermia have shown that the threshold temperature and latency of GCs were significantly lower in insulted pups than in controls [11].

However, the classical use of thermometers of different types, such as internal rectal electrodes, implantable probes or external infrared paw and tail sensor clips can be quite stressful for the animals. These devices can cause incontrollable variability in data acquisition that may partly hide the true effects of a treatment. Therefore, the development of non-invasive ways to measure the animal core temperature generates tremendous interest in this field of research. Using real-time thermographic images represents a promising advantage in that context by eliminating stressful probes and unnecessary physical manipulations of the animals for physiological measurements in the subjects and by getting more accurate estimates of possible differences between experimental conditions and treatments. Thus, in an ideal scenario, it is very important to be able to monitor accurately the temperature of the subject regularly without disturbing it during the experiment.

An efficient way to obtain a large amount of data for this experiment is to use a thermographic camera that performs temperature measurement at 30 Hz. Every pixel of an image obtained with a thermographic camera corresponds to a temperature measurement. By selecting in each frame the pixels that correspond to the body of a subject, it is then possible

to get continuous temperature measurement of the animal. The challenge of this work is thus to select pixels on the body of a subject every f frames in the context of hyperthermia experiments mimicking fever-induced atypical febrile seizures. However, the context of hyperthermia adds the challenge that the temperature of the environment changes with respect to the temperature of the animal, and, at some point, the temperature of the animal is essentially the same as its environment.

Some researchers have studied automatic monitoring of the temperature of subjects. Notably, in the work of [12], thermographic images of the faces of six patients were acquired every hour and during seizure events as indicated by real-time EEG analysis. Thermal images were filtered manually to remove images where occlusion occurred. Since the face was in the middle of the image, the temperature measured was the maximum in the center region and there were no tracking requirements. Tracking is required to detect and localize a moving subject in an image. Tracking was performed in the works of [13, 14, 15] to measure the temperature of a moving subject. In [14], a mean-shift tracker and a model based on the histogram of initial body temperature were used for tracking a shaved patch on the body of a rat. [13] and [15] instead used a particle filter tracker that models the shaved patch using edges around the patch and the mean intensity. Although these methods performed well enough for their intended body temperature measurement application, they are not applicable to our problem because of the low contrast between the body and its environment. The images that we process lack strong edges and present a uniform appearance. Recently, [16] proposed a tracking method based on level sets to track multiple rats in infrared images. The method assumes a large contrast between the animal and its environment. Recently, [17] proposed a method to track a rat in low-contrast thermographic images and measure the animal temperature. The animal is tracked by merging motion pixels to the previous rat

area and by morphological operations to clean up the animal area. The method is not robust enough in animal localization and the temperature obtained is not stable enough.

In this paper, we propose a novel method to detect and select, in each frame of a thermographic video, pixels that correspond to an area on the animal. Our method is based on the minimization of a cost function that uses temperature smoothness, proximity, area, and motion to determine the best candidate region among regions extracted using a temperature-based segmentation. Pixels in the candidate region are then selected for body temperature estimation.

The paper is structured as follows. Section 2 presents our materials and methods, section 3 presents validating experiments and section 4 concludes the paper.

2 Material and methods

2.1 Animal subjects and housing

Two pregnant (non-primipara) Sprague-Dawley female rats precised on embryonic day 10 (E10) were obtained from Charles River laboratories (St. Constant, QC, Canada) and used in this study. After thirteen days of environmental habituation to facilities by the mothers (i.e. till partuation), 19 newborn rats (6 females and 13 males) were randomly assigned for a hyperthermia-induced seizure paradigm (HS) occurring 10 days later. Rat pups were kept with their mother until P10 and housed in a 12 hour light/dark cycle with free ad libitum access to milk, food and water. The dam and pups stayed undisturbed in the animal facility except for the periods of cage maintenance (once a week, less than 10 minutes). All procedures for the use and care of animals conformed to policy and guidelines of the Canadian Council for Animal Care (CCAC), and the protocols were approved by institutional rules

from the Comité Institutionel des Bonnes Pratiques Animales en Recherche (CIBPAR) at the CHU Ste-Justine Research Center, Université de Montréal.

2.2 P10 Hyperthermia-induced seizure paradigm

In all litters when pups reached postnatal day 10 (P10), they were exposed to HS as previously described by [11] and adapted from [18, 11, 5, 3, 6, 8, 9]. All experiments started at around 1 PM, the dam was retired and the offsprings weighted. Then, each pup was individually placed in a Plexiglas box ($30cm \times 30cm \times 30cm$ with 32 $7mm$ wide small holes, 8 on each sides excluding top and bottom pannels) in which the initial temperature inside the box was approximately 23^oC. During the hyperthermia experiements, a hair-dryer produced an airflow, progressively heating the content of the box to increase the core temperature of the rats to 44-47 ^oC externally (corresponding to 40,5-43,5 ^oC internally (see figure 3)) over a period of 8 to 11 minutes. Each pup remained in the box until the onset of a generalized convulsion (GC) (i.e. tonic-clonic seizure with loss of posture) was observed. Just after the GC, they were immediately removed from the box and sacrificed for other purposes [7].

2.3 Data acquisition

To acquire the videos, a window was pierced in the cover of the box to insert the camera lens (10 cm in diameter). The videos have a resolution of 320×240 and are grayscale (each tone of gray correspond to a specific temperature). All videos were taken at about 29.4 frames per second. The thermographic camera (FLIR Thermovision A40M) was set with a linear scale between 20 and 53^oC. According to its specification, the thermographic camera has a precision of 0.08^oC. In these experiments, we pooled, as a whole, both data from male and female rats to account for possible physiological variations.

2.4 Problem definition and principles of our proposed method

At the beginning of the experiment, the subject can be easily segmented from the background with simple thresholding because it is hotter than its environment, as shown in Figure 1(a). As the temperature inside the box increases, the rat's temperature becomes very similar to the temperature of the box' floor, as shown in Figure 1(b). Then, a temperature inversion occurs and the rat's temperature is lower than the temperature of the box' floor, as shown in Figure 1(c and d). In these two latter cases, tracking the rat is difficult because of low image contrast (the contrast is less than 20 gray levels, or 2.5 ^{o}C). The rat sometimes urinates, which creates low temperature spots that slowly dry out, and generate apparent motion, as shown in Figure 1(a and b). Furthermore, to protect the extremities of the animal, a protective aqueous gel lotion is used, which acts at the beginning of the experiment as a thermal isolator (see the darker part of the animal in Figure 1(e)). Lastly, when the animal stays still for a period of time, the part of the floor under it becomes at the same temperature. When the rat then moves, it creates a ghost-like rat region. That is, there is a region on the floor that has briefly the same temperature and the same shape as the rat.

[Fig. 1 about here.]

The combination of low contrast, temperature inversion, protective lotion, ghosts, and continuous temperature variation of the subject and of the background preclude the use of simple thresholding or classification by training. We postulate that tracking is required to localize the animal. Once the rat's position is determined, its external body temperature can be estimated, which is the ultimate requirement for this experiment.

Given the conditions stated above, and first assuming perfect location at every frame, our proposed method was designed based on the following principles:

1. If no motion is detected, the temperature should be measured in the same area as for the previous frame. Here, we assume that motion is mostly caused by the rat's movements. If the rat was previously localized correctly, for measurement stability, we should measure at the same position;
2. If there is motion, the location of the animal should be re-evaluated. In that case, we should update the rat's region by selecting pixels that are nearby (the rat cannot move very far instantaneously), that are at similar temperatures (the temperature of the animal changes smoothly), and that give rise to a region of a size similar to the rat (the rat has always more and less the same size).

In practice, the location of the animal may be wrong and cannot be garanteed. This can happen when there is an area close to the animal that has a similar shape and a similar temperature, such as a ghost after the rat was motionless, or when the animal and the environment have similar temperatures. Because of principle 1, we will measure the temperature in the wrong position as long as the rat does not move. Even worse, motion in the ghost area or in a region with a similar temperature as the rat's (e.g. wiggling rat's tail or drying urine) may cause incorrect location due to principle 2, if that region meets all the selection criteria. Thus, to recover the track of the rat region and to strengthen principle 2, we use a third principle:

3. If the bounding box of the motion pixels encompasses a region of a size similar to the rat's, add this region to the possible measurement region.

We assume that if the bounding box of the motion pixels corresponds to the size of the rat, it means that the whole body of the animal is moving in a particular direction, and thus it is a strong indication of the position of the animal, i.e. the animal should be in the middle of that bounding box.

These principles are integrated in our temperature measurement methodology using a cost function, as detailed in the next section.

2.5 Animal localization by minimization of a cost function

To localize the animal when there is motion (principle 2), we select a candidate region R^a that minimizes a cost function defined as

$$R^a = \min_{R^i \in R} \left(A\Delta_T^{R^i} + B\Delta_S^{R^i} + C\Delta_D^{R^i} \right), \tag{1}$$

where A, B, and C are weights, R is a set of candidate regions, and

$$\Delta_T^{R^i} = \left| T^{R^i} - T_{prev} \right|, \tag{2}$$

where T^{R^i} is the temperature of the region R^i and T_{prev} is the temperature of the animal in the previous frame, and

$$\Delta_S^{R^i} = \left| S^{R^i} - S_{prev} \right| / \max(S^{R^i}, S_{approx}), \tag{3}$$

where S^{R^i} is the area of region R^i, S_{prev} is the area of the animal in the previous frame, and S_{approx} is the approximate area of the animal, and

$$\Delta_D^{R^i} = \left| P^{R^i} - P_{prev} \right|, \tag{4}$$

where P^{R^i} is the center position of R^i and P_{prev} is the center position of the animal in the previous frame.

That is, Eq. 1 selects the region R^i among a set of candidate regions R that is close, of the same size, and at the same temperature as the region in the previous frame. The set of

regions R is built by segmenting the image into two categories: 1) The pixels that are within α standard deviations from T_{prev}, and 2) the pixels that are not. R is made of the connected components R^i that are in the first category. Each region R^i is thus made out of a subset of pixels that are at about the same temperature value as the previous animal region. This allows us to enforce smoothness in temperature from one frame to the next. Because a single value of α does not always allow obtaining the real rat region, R includes R^i obtained with a range of α value.

Using principle 3, we also add in R the bounding box of the motion pixels. At time t, motion pixels I_M^t are pixels such that:

$$\forall (x,y) \in I_M^t, \left| I^t(x,y) - I^{t-1}(x,y) \right| > \varepsilon, \tag{5}$$

where $I^t(x,y)$ and $I^{t-1}(x,y)$ are video frames at time t and $t-1$, and ε is a threshold to remove noisy pixels that do not correspond to any motion and to remove small changes due to the heating of the environment. This value is preselected and kept constant for all frames. It is estimated based on the camera noise, which is approximately 2 or 3 intensity levels. We also remove isolated pixels. The resulting motion pixels correspond to large interframe differences only (rat motion, or urine).

The values of A, B, and C were selected based on experiments on one video ($rat101fs$, see section 3) by varying their values until the RMS temperature error (see Eq. 8) was minimized. These values are different for the region resulting from principle 3 (i.e., there is a second set of A, B, and C), and were selected in the same way. Since motion is a very strong indicator of the position of the animal, focus is put on $\Delta_S^{R^i}$. However, since this region does not precisely have the shape of the animal, it should not be unduly favored.

2.6 Initial subject area detection

At the beginning of the experiment, the subject's body is hotter than its environment. Simple thresholding may thus be applied. The initial subject area is the largest connected component R^a such that

$$\forall (x,y) \in R^a, I^1(x,y) > \tau, \tag{6}$$

where $I^1(x,y)$ is the intensity of a pixel of the initial frame of the experiment video at coordinates x and y, and τ is a threshold. R^a is the animal region at frame 1.

2.7 Temperature measurement estimation

Regardless of whether the animal was located correctly or not, estimating its temperature from a subset of pixels is a difficult problem because the body temperature is not uniform, and the thermographic measurements are sensitive to the orientation of the camera normal with respect to the normal of the surface being measured (the angle should be smaller than 35 degrees for proper measurement). This is illustrated by Fig. 2(a) and 2(b) that show an image of the temperature measurement on the rat's body and a histogram of the temperature distribution after conversion in Celsius.

[Fig. 2 about here.]

Because of the characteristics of thermographic cameras and of the body of the animal, we have chosen to estimate the body temperature of the animal with the mean of a 10×10 pixels area located in the center of the animal region. This favors selecting pixels that are oriented perpendicularly with respect to the camera sensor because we measure an approximately small flat surface on the back of the animal. Furthermore, selecting pixels in the

center of the animal region minimizes the risk of measuring background pixels. Recall that each pixel of a thermographic image is a temperature measurement. As such, we estimate the temperature of the animal with the mean of 100 measurements. Thus, the temperature at time t, T^t is

$$\begin{aligned} T^t = & T_{min} + \\ & \left((mean(I^t(x,y) \in R^a)/255) * (T_{max} - T_{min}) \right), \end{aligned} \tag{7}$$

where T_{min} and T_{max} are the minimum and maximum temperatures measured by the thermographic camera, respectively, corresponding to pixel intensities of 0 and 255. The scale was set to linear on the thermographic camera. T_{prev} corresponds to T^{t-1}. Note that the thermographic camera outputs are values between 0 and 255 representing temperatures based on the selected measurement range.

Now, since the animal location might not be perfect and because the animal's pose can vary, if a part of the animal is at least in the center of the area, we may expect to obtain body temperature estimations within a maximum error range of 1.5^oC. This expected measurement error was evaluated by randomly selecting a 10×10 pixels area on the animal's body, and by calculating the difference between the minimum and maximum mean body temperature estimation.

3 Experimental validations

To validate our proposed body temperature measurement method, we have processed the 19 hyperthermia videos. Regions R^i were obtained using α values between $0.4 \times \sigma_{T^0}$ and $2 \times \sigma_{T^0}$, where σ_{T^0} is the standard deviation of the initial temperature of the rat's body. For

R^i obtained using temperature segmentation, A, B, and C were set respectively to 3, 100, 0.7, and for R^i obtained using Eq. 5, A, B, and C were set respectively to 1, 150, and 0.5.

To evaluate our body temperature measurement method, we used the RMS error on the temperature as in previous works [17]. A partial ground-truth was generated by selecting one out of every 200 frames over the whole video sequence and by manually indicating the animal area. The temperature value was calculated as in Eq. 7. This gives a set of F ground-truth temperatures T_{GT}. Recall that our objective is to automatically select pixels corresponding to the animal to obtain an estimate of the temperature of its body. There is no real ground-truth for the body temperature based on the thermographic camera data. We simply aim at obtaining automatic body temperature estimates that are similar to the ones obtained by a human manually selecting the center of the body area of the animal.

Still, for four animals, we have investigated the relationship between our estimated external body temperature and internal temperature measured with a rectal thermal probe to establish the validity of our approach. These results are shown in Fig. 3. Initially, the internal temperature and the external temperature of the animal are about the same. As the temperature of the environment increases, the internal temperature and the temperature obtained with the thermographic camera become different, but they both increase at the same rate maintaining a gap of 4.3 ± 0.5^oC throughout the hyperthermia experiment. Thus, using a thermographic camera to estimate the evolution of the temperature of an animal in the hyperthermia context is a valid non-invasive approach. It is even possible to estimate the internal temperature from the external temperature with a small error.

[Fig. 3 about here.]

Now, for the evaluation of our proposed method, we compared the results obtained with our method with the results obtained manually by a human using F frames and the set of

temperatures T_{GT}. As mentioned previously, our first evaluation metric is the root mean square error defined as

$$T_{rms} = \sqrt{\frac{1}{F}\sum_{i=1}^{F}(T^i - T^i_{GT})^2}. \quad (8)$$

We selected this metric on temperature estimation error instead of using a metric on animal location accuracy, because the exact location of the animal is not required as long as the tracked animal area intersects to some extent with the actual rat position. That is, if the tracked area intersects with the animal area, some pixels on the animal will contribute to the body temperature estimation. As such, our method does not depend on the exact location of the animal. As demonstrated in section 2.7, we can consider that our method measures the temperature on the animal if it is within 1.5^{o}C from the ground-truth temperature. Otherwise, it measures the temperature elsewhere. Therefore, we use a second metric to validate our measurement region location, which is the number of tracking errors T_E defined as

$$T_E = \sum_{i=1}^{F}(\left|T^i - T^i_{GT}\right| > 1.5). \quad (9)$$

To separate the evaluation of major tracking errors from minor location errors, T_{rms} was calculated only for the F frames where T^i is within 1.5^{o}C from the ground-truth temperature. This is different from the methodology used in [17], where T_{rms} includes both major tracking and minor location errors (T_{rms} is calculated for all F frames). Let us first compare our results with the results of [17] using their evaluation methodology. Table 1 gives these results. For the 6 videos, our method gives a smaller RMS error. This indicates that our method locates more precisely the area corresponding to the animal. This is explained by the fact that temperature smoothness is used explicitly as a criteria to select the animal region (in the segmentation and in Eq. 1). Localization of the center of the animal is more accurate and the

subsets of pixels used for measurement are more homogeneous. Furthermore, the use of a motion-based animal area (principle 3) allows recovering more quickly from major location errors.

[Table 1 about here.]

Table 2 gives the RMS errors obtained with our method following our new evaluation methodology, and the number of tracking errors T_E. In the case where there are no major tracking errors, T_{rms} is between 0.3^oC and 0.7^oC from manual measurements by a human. Since selecting the appropriate subset of pixels on the animal is a difficult process, this result indicates that our method does not select the same pixel subset as the ones selected by a human because the centers of the tracked region do not correspond to the manually estimated centers. Therefore, we believe that our second metric better indicates the performance of our method. In about half of the videos, 90% of our method temperature estimations are close to a manual human estimation, and at worst, about 73% of our method temperature estimations are. This difference in performance is explained by many factors. First, the performance for the Rat1* videos is better than for the Rat2* videos, because for the Rat1* videos, the experiments did not use protective lotion. The protective lotion adds additional challenges in temperature measurement because a region with lotion looks colder in the thermographic image at the beginning of the experiments (see Fig. 1(e)). Although the center of the measurement area may correspond to the actual center of the animal, pixels with lotion will disrupt the temperature estimation. In fact, for Rat21dfs (14 errors out of 18), Rat21hfc (13 errors out of 15), Rat212ms (13 errors out of 14), and Rat202ms (14 errors out of 17), most major tracking errors occur in the first half of the experiments where the lotion is highly perceptible by the thermographic camera. We can conclude that these previous tracking er-

rors are not related to location errors per se. A possible workaround would be to validate a measurement by verifying the homogeneity of the 10×10 pixels area.

[Table 2 about here.]

The other errors are caused by actual location errors. One type of error is related to the tracking of ghosts. If the rat moves away from a position it occupied for a long period of time, the tracking algorithm might measure the temperature of the ghost area. This is not dramatic in itself since the ghost-like region is at a temperature similar to the animal's. It is more problematic if this region includes urine. In that case, the same problem as with the lotion may occur. It is also problematic if the measurement region location is not updated (no motion) and the temperature is continuously measured at the ghost position. With time, the ghost position temperature rises to the environment temperature and deviates from the animal temperature. However, using principle 3, if the rat makes a large movement again, tracking will be recovered by way of the region obtained using Eq. 5. On the other hand, if the rat stays still, or does not move much, the tracker will stay in the wrong position, and we will get temperature measurements from the background. Finally, when there is large tail motion, the measurement region might be erroneously located to include a large part of the environment background. As shown in Table 2, and following the discussion of the previous paragraph, these actual location errors occur seldomly (about 10% of the time).

4 Summary and conclusions

In this paper, we presented a method to measure the temperature of a body area of a rat in low contrast thermographic videos. Our proposed measurement method consists in tracking an animal to select pixels around its center to estimate its temperature. Our tracking method is based on the minimization of a cost function that uses constraints such as tem-

perature smoothness and proximity. Results show that for most of the time ($> 73\%$), we can successfully track the body of a rat for videos as long as 19000 frames to obtain temperature estimation within 0.7^oC of those obtained manually by a human. Furthermore, we have confirmed that the external temperature of the animal is linearly related to its internal temperature. Therefore, a thermographic camera allows properly studying animal temperature variations over time.

References

1. J. Engel. Intractable epilepsy: Definition and neurobiology. *Epilepsia*, 42:1528 – 1167, 2001.
2. J. Engel. Mesial Temporal Lobe Epilepsy: What Have We Learned? *Neuroscientist*, 7 (4):340–352, 2001.
3. S.A. Gibbs, M.H. Scantlebury, P. Awad, P. Lema, J. B. Essouma, M. Parent, L. Descarries, and L. Carmant. Hippocampal atrophy and abnormal brain development following a prolonged hyperthermic seizure in the immature rat with a focal neocortical lesion. *Neurobiol. Dis.*, 32(1):176 – 182, 2008.
4. A.S. Koe, N.C. Jones, and M.R. Salzberg. Early life stress as an influence on limbic epilepsy: an hypothesis whose time has come? *FNBEH*, 5(0):12, 2009.
5. M.H. Scantlebury, S.A. Gibbs, B. Foadjo, P. Lema, C. Psarropoulou, and L. Carmant. Febrile seizures in the predisposed brain: a new model of temporal lobe epilepsy. *Ann. Neurol.*, 58(1):41 – 49, 2005.
6. S. Gibbs, B. Chattopadhyaya, S. Desgent, P.N. Awad, O. Clerk-Lamalice, M. Levesque, R.-M. Vianna, R.-M. Rebillard, A.-A. Delsemme, D. Hebert, L. Tremblay, M. Lepage, L. Descarries, G. Di Cristo, and L. Carmant. Long-term consequences of a prolonged

febrile seizure in a dual pathology model. *Neurobiol. Dis.*, 43(2):312 – 321, 2011.

7. S. Desgent, N. Sanon, G.-A. Bilodeau, S. Duss, M. Salam, M. Sawan, and L. Carmant. Posnatal stress alters hyperthermic seizure patterns in a dual pathology rat model of epileptogenesis. American Epilepsy Society (AES) 65th annual meeting, Poster: 2.056, 2011.
8. S. Desgent, S. Duss, N.T. Sanon, P. Lema, M. Levesque, D. Hebert, R.-M. Rebillard, K. Bibeau, M. Brochu, and L. Carmant. Early-life stress is associated with gender-based vulnerability to epileptogenesis in rat pups. *PLoS ONE*, 7(8):e42622, 08 2012.
9. N.T. Sanon, S. Desgent, and L. Carmant. Atypical febrile seizures, mesial temporal lobe epilepsy, and dual pathology. *Epilepsy Res.Treatment*, 2012:1 – 9, 2012.
10. M.H. Scantlebury and J.G. Heida. Febrile seizures and temporal lobe epileptogenesis. *Epilepsy Res.*, (89):27 – 33, 2010.
11. M.H. Scantlebury, P.L. Ouellet, C. Psarropoulou, and L. Carmant. Freeze lesion-induced focal cortical dysplasia predisposes to atypical hyperthermic seizures in the immature rat. *Epilepsia*, 45(6):592 – 600, 2004.
12. S. Sunderam and I. Osorio. Mesial temporal lobe seizures may activate thermoregulatory mechanisms in humans: an infrared study of facial temperature. *Epilepsy Behav.*, 49(4):399–406, 2003.
13. A. Torabi, G.-A. Bilodeau, M. Levesque, J.M.P. Langlois, P. Lema, and L. Carmant. Measuring an animal body temperature in thermographic video using particle filter tracking. In *Advances in Visual Computing*, volume 5358 of *Lecture Notes in Computer Science*, pages 1081–1091. Springer Berlin / Heidelberg, 2008.
14. G.-A. Bilodeau, M. Levesque, J.M.P. Langlois, P. Lema, and L. Carmant. Thermographic body temperature measurement using a mean-shift tracker. In *The International Conference on Bio-inspired Systems and Signal Processing (BIOSIGNALS 2009)*, pages

18 –24, 2009.

15. G.-A. Bilodeau, A. Torabi, M. Levesque, C. Ouellet, J.M.P. Langlois, P. Lema, and L. Carmant. Body temperature estimation of a moving subject from thermographic images. *Mach. Vision Appl.*, 23:299–311, 2012.
16. M. Mayya and C. Doignon. Visual tracking of small animals based on real-time level set method with fast infra-red thermographic imaging. In *Robotic and Sensors Environments (ROSE), 2011 IEEE International Symposium on*, pages 60 –64, 2011.
17. G. Bilodeau, R. Ghali, S. Desgent, J.M.P. Langlois, R. Farah, P. St-Onge, S. Duss, and L. Carmant. Where is the rat? tracking in low contrast thermographic images. In *Computer Vision and Pattern Recognition Workshops (CVPRW), 2011 IEEE Computer Society Conference on*, pages 55 –60, 2011.
18. T. Z. Baram, A. Gerth, and L. Schultz. Febrile seizures: an appropriate-aged model suitable for long-term studies. *Dev. Brain Res.*, 98(2):265 – 270, 1997.

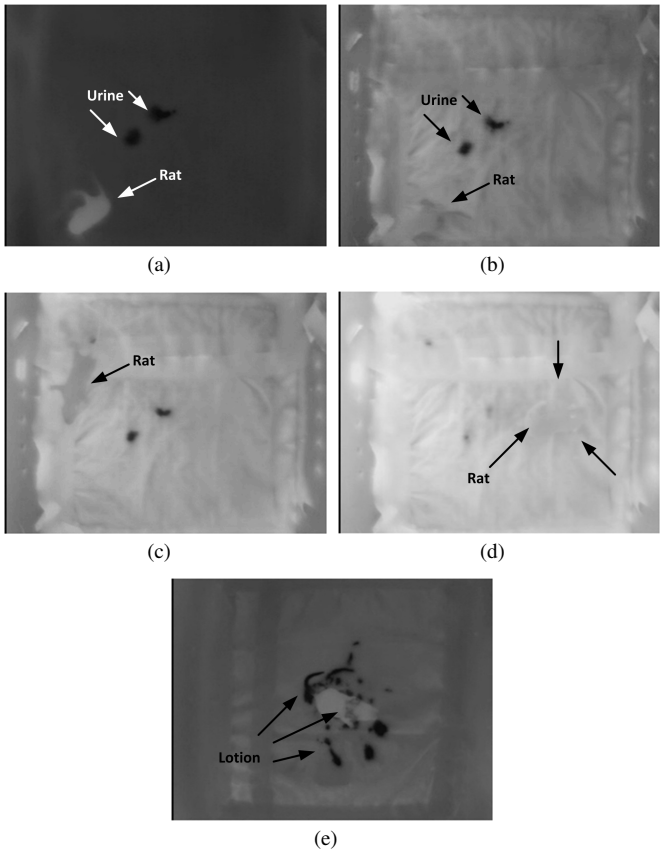

Fig. 1 Animal to track at different frames during experiments. a) At the beginning of the experiment (animal hotter than background), b) close to the moment of temperature inversion, c) after temperature inversion (animal colder than background), d) by the end of the experiment (just before the occurrence of the GC and loss of the righting reflex), and e) the effect of protective lotion.

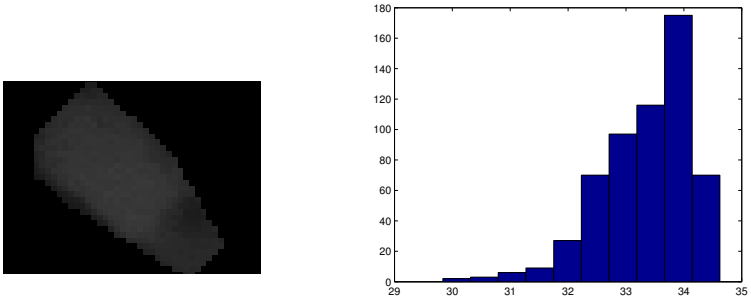

(a) (b)

Fig. 2 Typical temperature measurement on the body of an animal. a) zoom on a thermographic image of the body of a rat, and b) temperature histogram (in Celsius) of the pixels on the body of the rat.

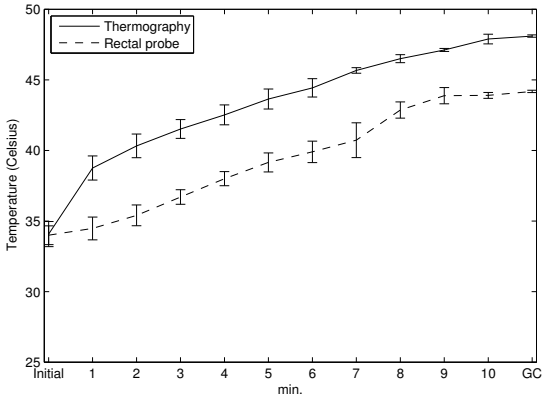

Fig. 3 Comparison of the evolution of animal temperatures by thermography and by a rectal probe. GC in the graph stands for the moments in time when the animals have generalized convusions.

Table 1 RMS temperature errors in ^{o}C obtained for 6 videos using the evaluation methodology of [17]

Video name	# Frames	F	T_{rms} [17]	T_{rms} (Our)
Rat101fs (Rat1)	10222	52	0.68	0.41
Rat108fc (Rat8)	8310	42	0.67	0.47
Rat10bms (Ratb)	15174	75	0.78	0.70
Rat10cms (Ratc)	16752	84	1.62	0.77
Rat10dmc (Ratd)	9831	47	1.43	0.65
Rat10fmc (Ratf)	11181	55	0.90	0.82

Table 2 RMS temperature errors in ^{o}C obtained for 19 videos

Video name	# Frames	F	T_{rms}	T_E	% T_E
Rat101fs	10222	52	0.33	1	1.92
Rat108fc	8310	42	0.32	2	4.76
Rat10bms	15174	75	0.42	4	5.33
Rat10cms	16752	84	0.44	6	7.14
Rat10dmc	9831	47	0.48	2	4.26
Rat10fmc	11181	55	0.62	6	10.91
Rat21cfs	16942	83	0.58	10	12.05
Rat21dfs	15827	76	0.59	18	23.68
Rat21gfc	14719	68	0.65	8	11.76
Rat21hfc	14229	70	0.59	15	21.42
Rat211ms	19334	96	0.59	8	8.33
Rat212ms	16122	76	0.64	14	18.42
Rat214mc	12822	61	0.59	8	13.11
Rat215mc	8880	44	0.70	11	25.00
Rat201ms	12749	64	0.57	3	4.69
Rat202ms	12453	62	0.67	17	27.42
Rat203mc	13018	66	0.49	1	1.51
Rat204mc	13079	65	0.57	7	10.77
Rat205mc	14180	71	0.49	2	2.82